ACS OMEGA

Article

http://pubs.acs.org/journal/acsodf

Self-Reducing Copper Precursor Inks and Photonic Additive Yield Conductive Patterns under Intense Pulsed Light

Yitzchak S. Rosen,[†] Alexey Yakushenko,*[,‡] Andreas Offenhäusser,[‡] and Shlomo Magdassi*[,†]

[†]Casali Center of Applied Chemistry, Institute of Chemistry, The Hebrew University of Jerusalem, Jerusalem 91904, Israel

[‡]Institute of Bioelectronics (PGI-8/ICS-8) and JARA—Fundamentals of Future Information Technology, Forschungszentrum Jülich, 52425 Jülich, Germany

Supporting Information

ABSTRACT: Printing conducting copper interconnections on plastic substrates is of growing interest in the field of printed electronics. Photonic curing of copper inks with intense pulsed light (IPL) is a promising process as it is very fast and thus can be incorporated in roll-to-roll production. We report on using IPL for obtaining conductive patterns from inks composed of submicron particles of copper formate, a copper precursor that has a self-reduction property. Decomposition of copper formate can be performed by IPL and is affected both by the mode of energy application and the properties of the printed precursor layer. The energy application mode was controlled by altering three pulse parameters: duration, intensity, and repetitions at 1 Hz. As the decomposition results from energy transfer via light absorption, carbon nanotubes (CNTs) were added to the ink to increase the absorbance. We show that there is a strict set of IPL parameters necessary to obtain conductive copper patterns. Finally, we show that by adding as little as 0.5 wt % single-wall CNTs to the ink the absorptance was enhanced by about 50% and the threshold energy required to obtain a conductive pattern decreased by ~25%. These results have major implications for tailoring inks intended for IPL processing.

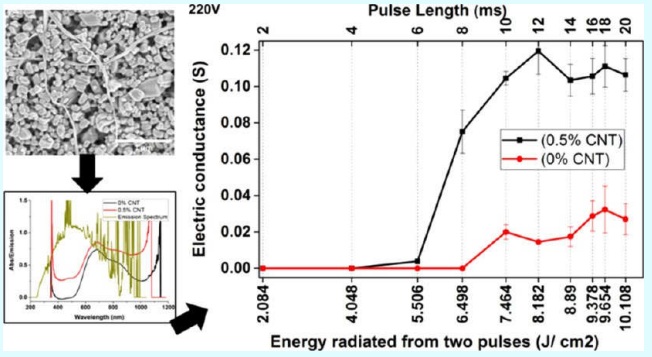

1. INTRODUCTION

Printing electrical conductive interconnections is a key component in the field of printed electronics. Conducting components are usually printed, followed by a post-printing step that usually involves heating to sinter or decompose the printed conducting element. In the past few years, several new approaches for post-treatment of conductive inks have been reported, including methods such as photonic curing, plasma exposure, and laser selective sintering. Each method has advantages; for instance, laser selective sintering enables direct local reduction and sintering[1,2] to form very fine electrical wiring without the need for a conventional printing step, or it can be used to form flexible transparent films by welding copper nanowires.[3−5] In comparison, photonic curing is a rapid and scalable process that can be used to treat large surface areas simultaneously. The main advantage of the latter method is that only printed patterns are affected; thus, there is no wastage of material compared to that in laser sintering in which the unsintered material is washed away.

Photonic curing employs intense pulsed light (IPL), which is much faster than traditional thermal heating and laser selective sintering, and therefore is suitable for roll-to-roll (R2R) processes with plastic substrates. In the IPL method, a xenon lamp irradiates a wide area at once, using a short and powerful light pulse in the UV−vis−IR range. The IPL method causes rapid heating of a thin layer of material, which is exposed to the light pulse.[6] As only the exposed surface is heated, the bulk of the substrate on which the sample is printed remains unaffected. Shortly after the pulse is applied, the heat from the affected thin surface dissipates into the thicker substrate layer, resulting in fast cooling of the printed layer. The local heating can induce sintering of metal nanoparticle (NP) inks[3,7−10] or thermal decomposition of copper precursor inks. This enables the use of IPL for obtaining conductive patterns. Copper precursor inks include two types of inks: those with inorganic precursors[11−13] that contain a reducer, and metal-organic decomposition (MOD) inks[14,15] that in most cases do not require addition of a reducer. IPL can be used for decomposition of copper precursors without the problems associated with conventional oven heating (e.g., without the need for a nitrogen environment to prevent copper oxidation).[9]

Typical MOD inks contain a low concentration of copper; therefore, their utilization in printed electronics is limited to printed conductors with little copper content. Previously reported MOD inks contain metal complexes that are dissolved in a solvent and usually have a low metal loading (ca. 10−15 wt

Received: December 7, 2016
Accepted: February 3, 2017
Published: February 16, 2017

DOI: 10.1021/acsomega.6b00478
ACS Omega 2017, 2, 573−581

%). This limits their printing efficiency to obtaining conductive patterns with high metal content and thus they may require multiple printing stages and excessive removal of solvents after each printing stage.

We have developed a new ink that is composed of submicron particles of copper formate with a high metal loading[16] that is stable to oxidation and is prepared by a very simple method that is common in the conventional printing industry. Unlike the reported MOD inks, this new ink is composed of a dispersion of copper salt particles. This new ink actually has the advantages of the present reported approaches without their inherent disadvantages: copper NP inks with high metal load, which suffer from oxidation, and oxidation-stable MOD inks, which suffer from low metal load. Upon decomposition of this copper salt, the Cu^{2+} ion is self-reduced to a conducting Cu^0 form. Thus, unlike that for other particle-based precursor inks[12,13] to produce copper patterns, there is no need to add reducing agents to the ink formulation.

Decomposition of the salt precursor ink with photonic curing as done in this study occurs in two steps.[15] First, the copper salt absorbs light (in the 600−800 nm range), causing the excitation of electrons and local heating. Afterward, the rise in energy is sufficient to enable the decomposition of the copper formate to copper, carbon dioxide, and hydrogen, along with a reduction of the copper ion to pure copper by the formate counter ion. The general decomposition[17] reaction is presented as reaction 1 and the separate redox reactions[18] as reactions 2 and 3.

$$Cu(HCOO)_2 \xrightarrow{IPL} Cu_{(s)} + H_{2(g)} + 2CO_{2(g)} \quad (1)$$

$$Cu^{2+} + 2e^- \rightarrow Cu^0{}_{(s)} \quad (2)$$

$$2HCOO^- \rightarrow H_{2(g)} + 2CO_{2(g)} + 2e^- \quad (3)$$

One of the main disadvantages of photonic curing is the high energy consumption to generate the intense light pulses. Araki[15] et al. suggested that the most important factor in photonic curing is the absorbance properties of the ink. To enhance light absorbance and energy absorbance of copper formate patterns during photonic curing, we prepared a hybrid ink that contains copper formate particles and a very efficient light absorber. The latter material is carbon nanotubes (CNTs), which is known as the blackest material[19] with excellent light absorption,[20] electrical conductivity, and thermal conductivity. CNTs have been shown to have excellent solar−thermal conversion[21−23] and solar−thermal heating.[24] For example,[24] thin films of CNTs have been used to harvest and convert almost the entire incident solar light into heat for water heating and evaporation. As the emission spectrum from a xenon lamp is similar to the solar emission spectrum, it is reasonable to assume that the incident light from IPL will also be efficiently converted into heat by the CNTs. The generated heat can be evenly conducted along the CNT and can be transferred via direct contact to the surrounding copper formate particles, leading to their heating and decomposition.

In general, the available information concerning the use of IPL for decomposition of MOD inks is far from being systematic. There is no data on the effect of different pulse parameters on the electrical resistance and morphology of the obtained patterns, nor are there any examples for a practical approach to find the optimal IPL parameters for the decomposition of a MOD ink. Furthermore, the effect of enhancement of photoabsorption by addition of single-wall CNTs (SWCNTs) has not been reported before, and to our opinion, this will open an effective way to improve photonic curing processes.

In the present study, we used a PulseForge 1200 (NovaCentrix) system to show that copper formate-based inks can indeed enable printing conductive patterns without a need for reducing agents and inert atmosphere using the IPL process. Furthermore, we found that hybrid inks composed of both copper precursors and low concentration of CNTs enable a significant improvement in conductance due to more efficient light absorption.

2. RESULTS AND DISCUSSION

2.1. Investigating Pulse Parameters. The IPL system enables control of the pulse parameters, including duration and intensity. Each parameters' combination affects the energy flux profile and therefore affects the decomposition kinetics and the morphology of the obtained copper pattern. Figure 1 presents

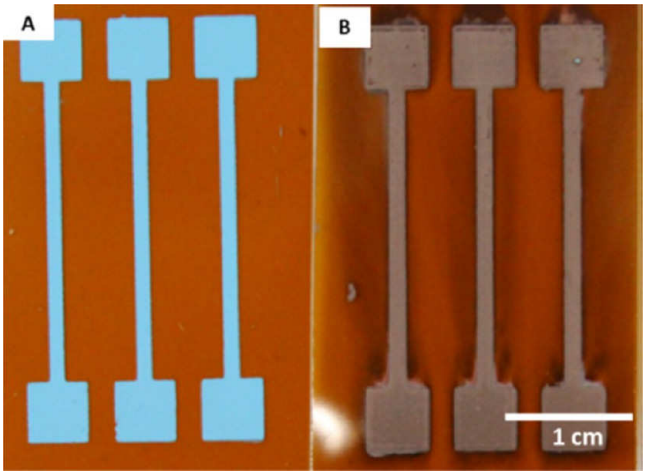

Figure 1. (A) Screen-printed copper formate pattern prior to decomposition. (B) Copper pattern obtained after decomposition with IPL (pulse parameters: two pulses, 240 V, 10 ms).

the visual outcome of typical experiments, in which a blue pattern is obtained by screen printing of the copper formate particle ink (resulting in a 13 ± 1 μm line height after drying, Figure 1A), and upon light irradiation, the blue color changes into a shiny reddish color, which is typical for copper metal (Figure 1B). Decomposition with IPL was performed in an air environment, and the copper ion was reduced by the formate (the reducing counter ion in the copper formate salt) to Cu^0. During decomposition, some soot is formed, and it can be seen as the shadow around the copper patterns. Qualitatively, the amount of soot formed is proportional to the pulse intensity and can be easily wiped away.

A methodical examination of the effect of pulse parameters on the decomposition of the copper formate particle ink was carried out by altering three key pulse parameters: the pulse duration in milliseconds (from 2 to 10 ms with 2 ms intervals), pulse intensity (controlled by the applied voltage to the xenon lamp from 180 to 450 V or less with 20 V intervals), and number of pulse repetitions at a frequency of 1 Hz (one to four repeats). To understand the effect of the different IPL parameter combinations on the decomposition of copper formate patterns, a screening experiment was performed with small segments of the pattern. The segments were methodically

DOI: 10.1021/acsomega.6b00478
ACS Omega 2017, 2, 573−581

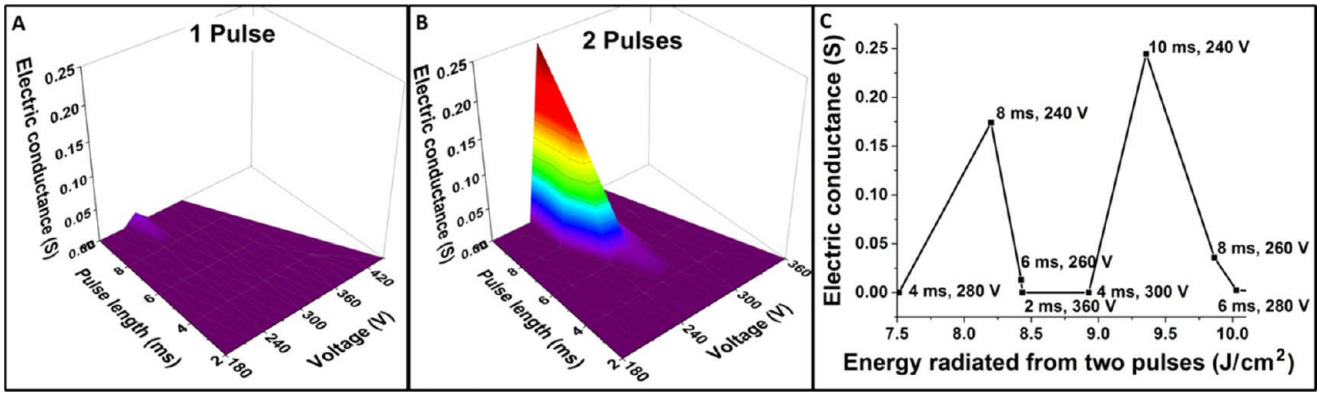

Figure 2. (A, B) 3D graphs; each graph displays the conductance measured in the screening experiment for all pulse voltage and duration combinations: (A) 3D plot of the combinations with one pulse and (B) 3D plot of the combinations with two pulses. (C) Conductance of the samples prepared with two pulses as a function of the total energy applied. The intensity and duration of the pulses for each data point are indicated.

treated with different IPL parameter combinations followed by resistance measurements. Figure S1 presents a typical sample used for the screening experiment; all segments in the sample were treated with two pulses with a duration of 10 ms and varying intensity. At a voltage of 180 V, the layer was unaffected; at 200 V, only partial decomposition was achieved; and at 220 V or higher, a copper pattern was obtained. The penetration depth depends on the pulse parameters and the thickness of the printed layer. In the samples in which there was only partial decomposition, we observed a layer of copper above a layer of copper formate. This shows that the energy applied was sufficient to decompose only the top layer but was not sufficient to penetrate to the lower part of the copper formate layer. The samples that were treated with pulse parameters that lead to full decomposition were found to contain pure face-centered cubic (FCC) copper throughout the whole layer, indicating that the light either penetrated fully or local heating of the upper layer caused the decomposition of lower layers.

The substrate, Kapton, has a visible orange color and absorbs light well in the 300−500 nm range. However, the contribution of the substrate light absorption to the decomposition of the samples is insignificant. This can be seen by visual inspection of the said partially decomposed samples; if sufficient heat had been transferred from the substrate to the copper formate to induce decomposition, we would have seen samples with decomposition adjacent to the substrate. In practice, in all samples that were only partially decomposed, it was visible that there was a layer of copper above the layer of copper formate. Furthermore, initial experiments with samples on a transparent polyethylene naphthalate (PEN) substrate had similar results in terms of minimal pulse parameters needed to induce decomposition. Thus, it was evident that the energy needed for decomposition was obtained directly from the light pulse to the printed copper formate layer and not via substrate heating.

Figure 2A,B presents two 3D graphs showing the conductance obtained with different pulse parameters in the screening experiment. Only very specific combinations resulted in a conducting copper pattern. Figure 2A, which plots the conductance obtained from various pulse combinations with a single pulse, shows that a single pulse does not lead to conductive samples, except for one combination (240 V, 10 ms) that results in low conductance. A comparison between the conductance obtained by one pulse and that obtained by two pulses (Figure 2B) shows that in general higher conductance is obtained with two pulses. Conductive samples were obtained only by treatment with more than one pulse, in which each pulse was formed at a voltage range of 220−260 V and with a pulse duration above 6 ms. The best conductance, 0.244 S (line length: 2.5 mm), was measured for two pulses at 240 V and 10 ms duration. From these results, it is clear that the patterns composed of copper formate particles can indeed be converted into conductive patterns by the IPL exposure (the 3D graphs for three and four pulses were comparable to the graph for two pulses, as presented in Figure S2). Furthermore, for the combinations of low pulse intensity and low pulse duration, the photonic curing did not lead to decomposition or led only to partial decomposition of the copper formate layer. High-voltage pulse combinations led to the release of a substantial amount of soot, resulting in a black sediment around the copper pattern. Therefore, even though decomposition of the copper formate occurred, the samples were not conductive.

It could be assumed that the governing parameter in obtaining conductivity is the amount of energy that is supplied to cause copper formate decomposition. Therefore, the energy supplied by the IPL process under the various parameters for a single pulse was measured by a bolometer. Surprisingly, it was found that there was no straightforward correlation between the supplied energy and the obtained conductance. Figure 2C presents the data from the screening experiment from a different point of view, by examining the conductance of the samples prepared with two pulses as a function of the applied energy. All conductive samples were those that were treated with long pulses (6−10 ms), whereas shorter pulses did not result in a conducting sample, even in the cases in which the total energy was higher than that of the long pulses. This finding was also observed for three and four pulses. Therefore, we conclude that while using IPL for the decomposition of copper formate, the way in which the energy is applied is more important than its net total value. The duration of the pulse is a critical parameter; longer pulses can lead to better results. This conclusion is similar to the observation by Niittynen[7] regarding the IPL treatment of copper NPs. Thus, the way in which the energy is applied is important in both a system that requires mainly sintering (of the copper NPs) and, as we show, a system that requires decomposition of a precursor.

After finding the best pulse parameters to obtain conductance (two pulses, 240 V, 10 ms), an additional experiment was conducted for a larger-area pattern, 1.3 × 22 mm^2, in which the conductance was 0.039 ± 0.007 S. Figure 3A

DOI: 10.1021/acsomega.6b00478
ACS Omega 2017, 2, 573−581

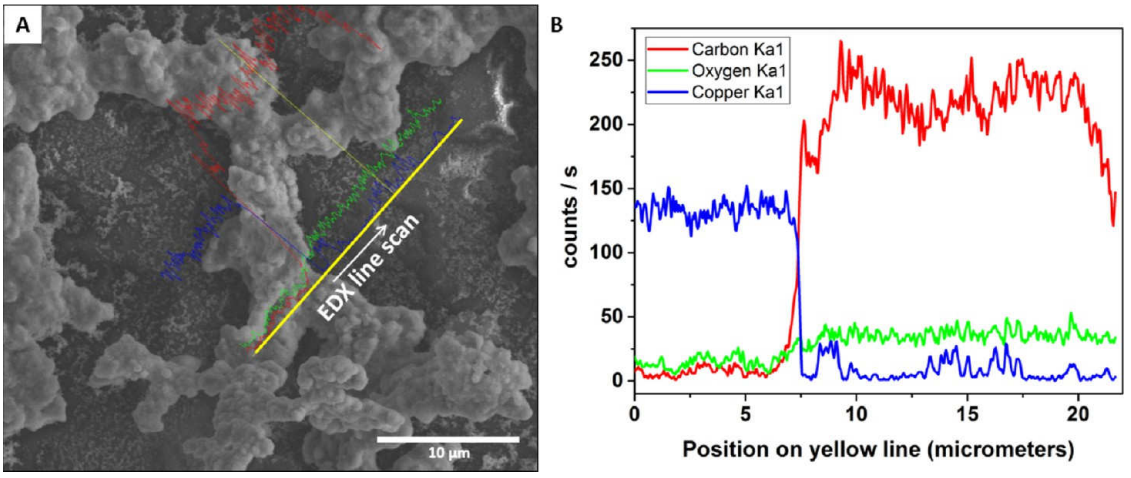

Figure 3. (A) SEM image of a sample prepared with two 240 V, 10 ms pulses. An EDX line scan was performed on the sample; the scanned line is marked by the thick yellow line, and the result is plotted above the yellow line and enlarged in the EDX line scan (B) showing the locations of copper, oxygen, and carbon along the yellow line in (A).

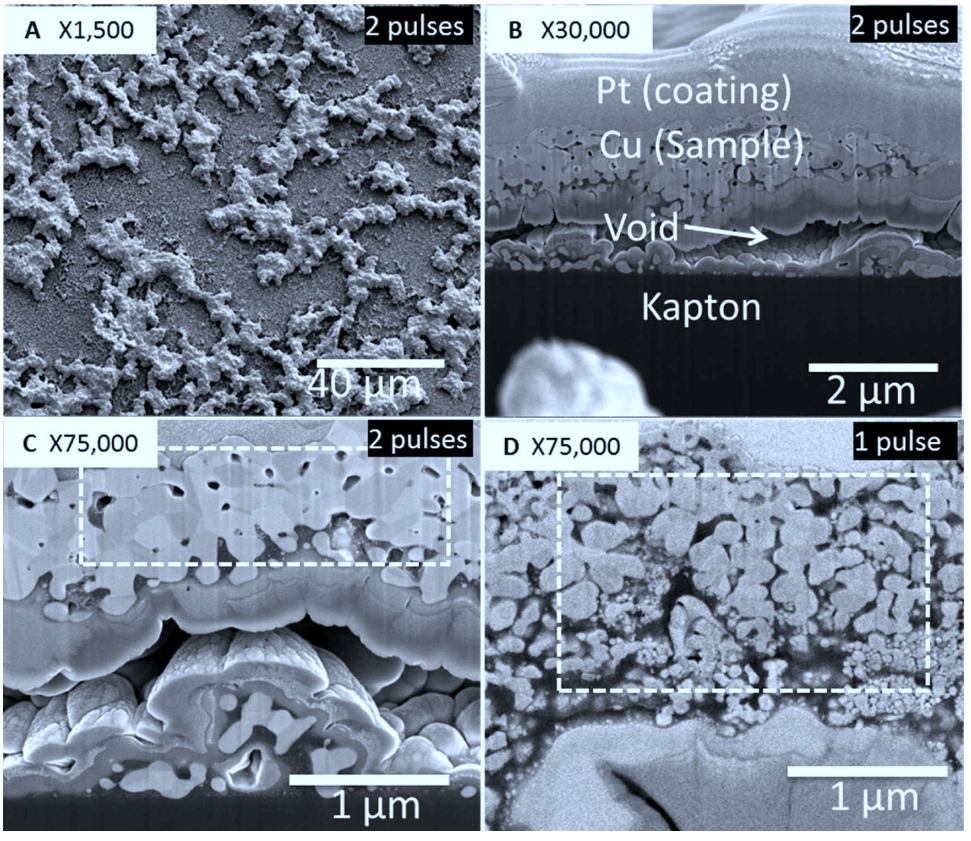

Figure 4. (A–C) Images of a sample treated with two pulses of 240 V, 10 ms. (A) Top-view SEM image. (B, C) Cross-sectional images at increasing magnifications, showing hollow "voids" inside the copper layer. (D) Cross-sectional image of a sample treated with 1 pulse of 240 V, 10 ms.

presents a scanning electron microscopy (SEM) image of the sample showing an "island" morphology of the pattern. An energy-dispersive X-ray (EDX) line scan (Figure 3B), with the prevalent atoms displayed along the yellow line in Figure 3A, shows that the islands are mainly composed of copper, whereas the areas between the islands contain mainly carbon and oxygen. It should be noted that as the sampling depth of the EDX is over 0.5 μm it is possible that the detected carbon and oxygen originate from the underlying Kapton substrate and not from copper formate or copper. Because of the nonhomogeneous copper morphology, we were unable to calculate the conductivity of the samples.

A closer look at the film morphology was taken with the cross-sectional images obtained by focused ion beam (FIB). Figure 4A shows the top view of the sample, and Figure 4B,C presents the cross-sectional images at various magnifications of the sample prepared with two pulses (240 V, 10 ms). The most interesting feature is that there are elongated voids inside the copper layer. Most probably, these voids result from the release of gases during the decomposition of copper formate (see

DOI: 10.1021/acsomega.6b00478
ACS Omega 2017, 2, 573–581

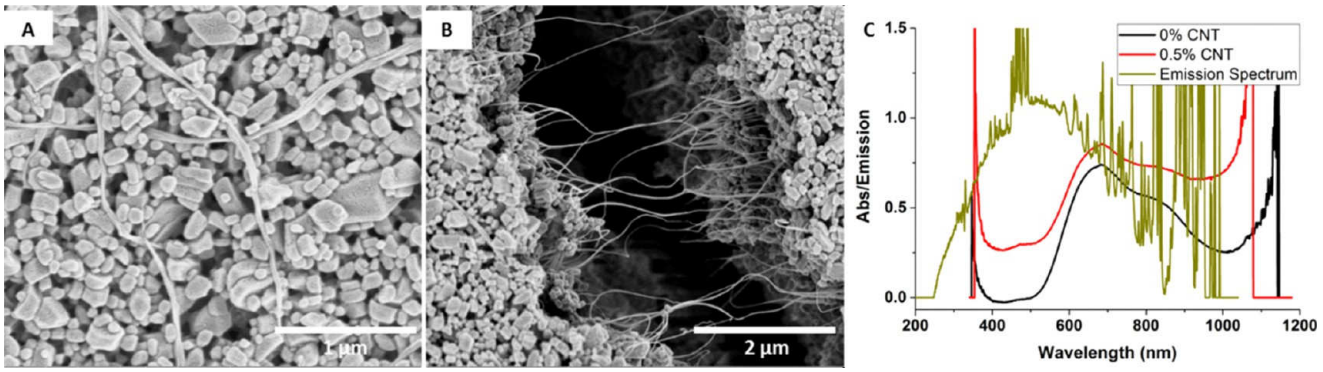

Figure 5. (A) SEM image of the hybrid ink before decomposition. Single CNTs (or several in a bundle) are spotted on the surface of the printed layer. The particles around the CNTs are copper formate particles. (B) CNTs found in the cracks of the ink layer that were formed during preparation of the sample for SEM. (C) Light absorption spectra of the inks with and without CNTs, along with the normalized emission spectrum of a single light pulse.

reaction 1). It should be noted that a "pop" sound can be heard during the IPL process, which is due to either the instantaneous release of gases during decomposition or the bursting of the voids. In addition, when the light interacts with the top layer of the printed pattern, it is possible that the upper layer decomposes first to form a copper film, and when the lower layer decomposes, the released gas is captured under the previously formed copper film, thus forming the voids. These voids probably also negatively affect the adhesion of the metal to the substrate, and this should be further improved. These findings support Araki's[15] hypothesis that morphological defects are formed due to the release of carbon dioxide gas during photonic curing of various copper complexes.

Microscopic examination of the samples prepared in the screening experiment can shed light on the role of each of the two pulses needed to obtain a conductive line. From the cross-sectional images of the samples prepared with a single pulse (Figure 4D) compared to those of a sample prepared with two pulses (Figure 4C), it is evident that a single pulse causes the decomposing of the copper salt, whereas the second pulse causes sintering and densification of the formed copper particles (area marked by dotted squares). X-ray diffraction (XRD) measurements of the samples obtained with one and two pulses (pulse parameters: 10 ms, 240 V) indicate that in both cases only crystalline copper is present; thus, it is possible to conclude that the copper formate was fully decomposed by the first pulse.

After the first pulse that decomposes the copper formate to copper, the optical properties of the pattern change. Copper NPs absorb light in the 200−600 nm range;[25] thus, there is an overlap with the emission spectrum from the IPL and copper particles; therefore, the IPL should also contribute to sintering of the copper particles formed, as previously reported.[7,26]

A theoretical calculation shows that the decomposition of copper formate into copper involves a ∼90% volume reduction; thus, when considering the island morphology, the film thickness reduction from 13 μm to about 2−4 μm is reasonable.

2.2. Hybrid Ink: Adding CNTs To Enhance Light Absorbance and Conductance. To improve the conductance of the printed patterns, we evaluated the possibility of increasing the light absorbance and, consequently, the total absorbed energy. We prepared hybrid inks, composed of copper formate particles, and CNTs, which are excellent light absorbers. In preliminary experiments, we found that the absorptance increases even at low concentrations of CNT. We present results from inks that contain 0.5 solid wt % SWCNTs. The CNTs were added to the copper formate powder and were well dispersed in the hybrid ink by the ultrafine wet grinding process. This concentration of SWCNTs was chosen as this was the highest that could be dispersed without significantly altering the viscosity of the dispersion during the grinding and dispersing stages, with the bead mill. We evaluated inks with a lower concentration of SWCNTs and found that the photonic absorbance is linearly proportional to the concentration of CNTs. Figure 5A presents single CNTs (or several in a bundle) on the surface of a printed pattern of the hybrid ink before decomposition. Figure 5B presents CNTs found in the cracks of the ink layer that were formed during preparation of the sample for SEM. The light absorption spectra of the inks (with and without CNTs) are presented in Figure 5C, along with the normalized emission spectrum of a single light pulse. As it can be seen, addition of 0.5 wt % CNTs (red line) enhances the light absorbance, especially in the 400−550 nm range, where the IPL is at its maximal light emission (olive green line) and the copper formate is at its lowest light absorption (black line). The absorptance in the main pulse emission range (300−700 nm) was calculated from the UV−vis reflectance spectra[15] to be 47.9 and 71.7% for the regular ink and hybrid ink, respectively. Thus, for wavelengths with strong emission from the IPL, the absorptance was enhanced by about 50% with the addition of as little as 0.5% SWCNTs. These results show that adding CNTs to the copper formate ink enables the utilization of a larger portion of the wavelengths emitted from the IPL, including the wavelengths that are not absorbed by copper formate.

A screening experiment, similar to the one presented in Figure 2A,B, was performed to compare the conductance values of the regular ink and hybrid ink after IPL irradiation with two pulses. According to the initial screening experiment, longer pulses resulted in better conductance; therefore, this screening experiment was conducted with a wider range of pulse durations, up to 14 ms. The 3D graphs are shown in the supplementary data (Figure S3A,B). The lowest energy supplied to the sample that resulted in partial decomposition was lower for samples with the hybrid ink than for those with the regular ink; this is to be expected because of the better light absorption. As with the regular ink, partial decomposition of samples with the hybrid ink was observed as a thin layer of copper above a layer of copper formate; thus, the energy applied was sufficient to decompose the top layer, but again, it

DOI: 10.1021/acsomega.6b00478
ACS Omega 2017, 2, 573−581

was not sufficient to penetrate to the lower part of the layer of copper formate with SWCNTs. Samples that were treated with the pulse parameters that lead to full decomposition were found by XRD to contain pure FCC copper without copper formate or copper oxides.

The optimal pulse settings to obtain conducting patterns for the two inks were different: For the regular ink, the best conductance for pulses with a duration of up to 12 ms was obtained with a voltage of 240 V and for longer pulses it was obtained with 220 V. For the hybrid ink, the best conductance was observed at 220 V for all pulse durations. Overall, by the preliminary screening experiment, it appears that the hybrid ink enabled obtaining printed patterns with a higher conductance than that obtained with the regular ink. After narrowing down the intensity parameters to 220 and 240 V (two flashes), we evaluated the samples with larger printed lines (22 × 1.3 mm^2 lines) under various pulse durations, from 2 to 20 ms with 2 ms intervals. For samples prepared at 220 V, the hybrid ink resulted in better electrical performance than that of the regular ink, whereas at 240 V, no significant difference was measured. In both sets of experiments, the samples with the hybrid ink required a lower energy threshold to obtain conductive patterns compared to that for those with the regular ink. Figure S3C,D presents the conductance for the samples prepared at 220 and 240 V.

Figure 6 presents the logos of the two research institutes printed on PEN, showing that the ILP process is also suitable

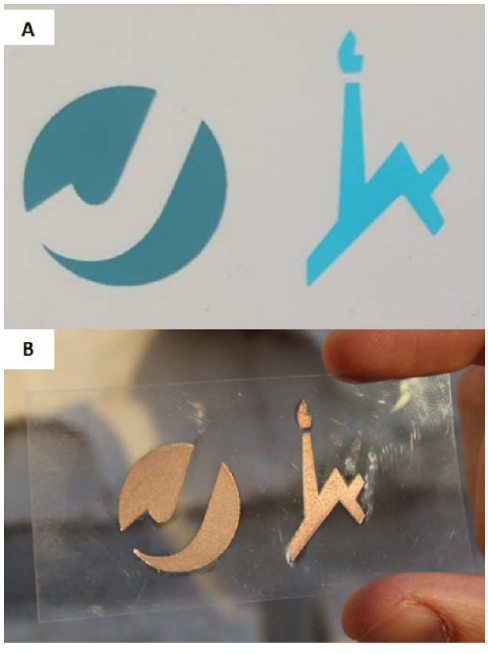

Figure 6. Printed logos of Forschungszentrum Jülich and HUJI with the hybrid and regular inks, respectively, on PEN (A) before decomposition and (B) after decomposition.

for large coverage patterns and for printing on other substrates. Figure 7 presents the average electrical conductance of large samples at 220 V, showing the significantly better results of the hybrid ink samples in terms of energy requirement and conductance. The lowest energy supplied to the sample that resulted in a conductive pattern with regular ink was 7.5 J/cm^2 (10 ms, 220 V), whereas for the hybrid ink, only 5.5 J/cm^2 (6 ms, 220 V) energy was required; thus, the required threshold

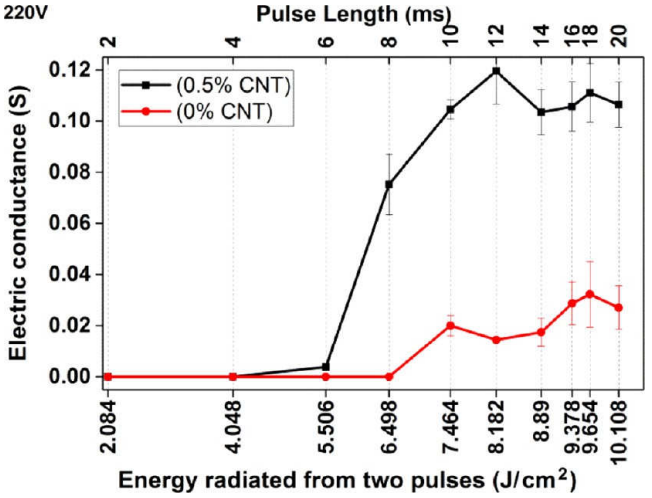

Figure 7. Average electrical conductance of three samples at 220 V for samples prepared with the regular ink and the hybrid ink.

energy decreased by 26%. The hybrid ink also resulted in better conductance values. For example, the conductance values of the samples with the regular ink were 0.02 ± 0.004 and 0.027 ± 0.008 S at 10 and 20 ms, whereas the conductance values of the samples with the hybrid ink were 0.104 ± 0.003 and 0.106 ± 0.001 S at 10 and 20 ms, respectively. Thus, the addition of 0.5 wt % CNTs improved the conductance 5-fold in these pulse parameters. To understand the difference in conductance, we examined the samples' morphology, as presented in Figure 8. When the inks were compared at both pulse durations, it was observed that the hybrid ink samples were more continuous with larger copper islands than the samples with the regular ink, thus explaining the better conductance obtained with the hybrid inks. At 240 V (see the image presented in Figure S4), there was no difference in morphology, and accordingly, the conductance of the regular ink samples was only slightly lower than that of the hybrid ink samples.

It should be noted that in addition to increasing light absorption, the CNTs may also act as conducting bridges between the copper particles and therefore improve the overall conductivity. This possibility is related to the findings of Hwang[27] who added activated MWCNTs to a copper NP ink to retain the conductivity during bending of copper patterns.

3. CONCLUSIONS

We present simple copper precursor inks that can be converted into conductive copper patterns by the IPL process. Unlike previously reported MOD inks, the presented inks are composed of a dispersion of copper salt particles that are stable to oxidation. We think that this approach will open the way to the development of a new family of MOD inks that can be implemented for a variety of metal precursors. Obviously, further optimization of the dispersion-type MOD inks will enable obtaining higher conductivity while using very high metal loads. We show that when the copper formate particle ink is used, the mode in which the energy is supplied is more important than the total energy supplied, whereas pulses with long durations are preferable for optimal results. This is similar to the findings[7] regarding the sintering of copper NPs with IPL. Furthermore, we found that the best conductivity was obtained with two pulses. The first pulse causes the decomposition of the

DOI: 10.1021/acsomega.6b00478
ACS Omega 2017, 2, 573−581

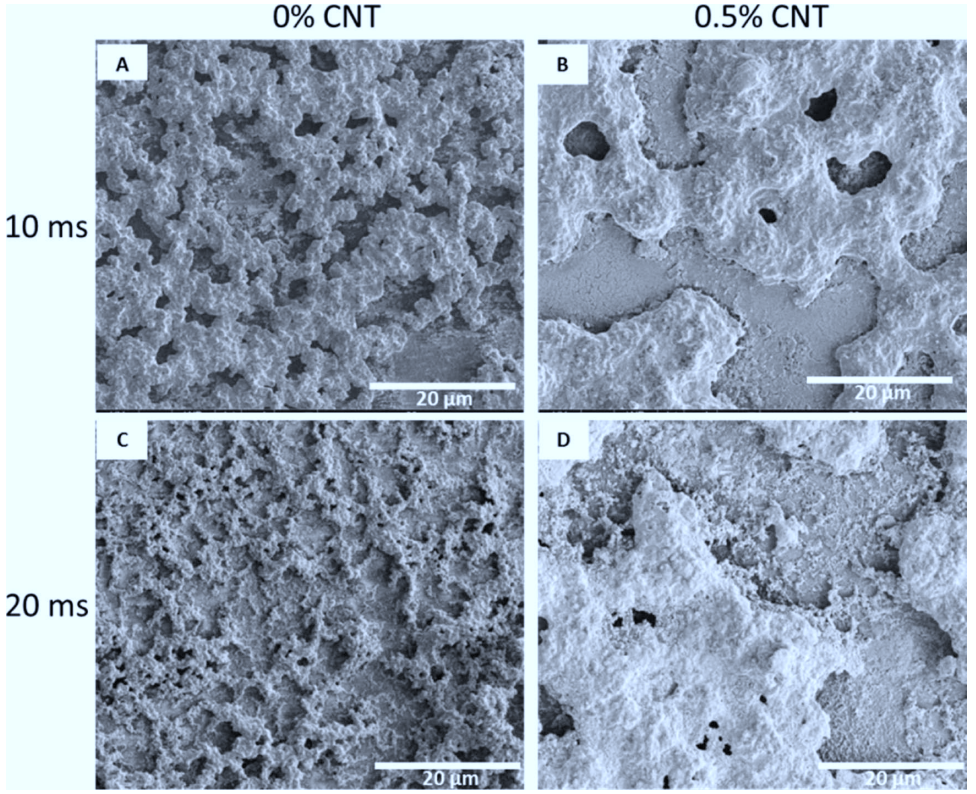

Figure 8. SEM images of samples after IPL irradiation with two pulses, each with an intensity of 220 V and pulse durations of 10 and 20 ms. (A, C) Regular ink without CNT. (B, D) Hybrid ink with 0.5 wt % CNT.

copper salt, whereas the second pulse causes sintering and densification of the copper particles formed.

Adding CNTs to copper precursor inks presents a new approach for improving the efficiency of photonic curing. The CNTs act as a photonic additive to induce energy absorption and may also function as a conductor that bridges the gaps in the copper film. As we show by morphology and conductance results, SWCNTs significantly improve the overall performance of the printed inks. This is the first time that CNTs have been used as light absorption enhancers to other conducting materials. These findings present a powerful approach that would enable expanding the IPL capabilities to materials that do not absorb light at convenient and commonly used wavelengths. The ability to tailor the material such that the pulses with lower energy will produce results similar to those from pulses with high energy should have economic implications for commercial production and use of the technology. As CNTs efficiently absorb light that is converted to heat, this heat is locally dissipated within the copper formate, thus inducing its decomposition. The lower illumination settings cause less heating of the substrate; therefore, the presence of CNTs may enable the use of more heat-sensitive substrates. We also expect that addition of photonic additives to conducting inks may lower the power consumption of IPL tools without compromising the conductivity. This method presents a viable approach to further decrease the costs in R2R processes.

4. EXPERIMENTAL PROCEDURES

4.1. Ink Preparation. *4.1.1. Preparation of Copper Formate Dispersion Ink.* Preparation of copper formate dispersion ink was described previously in ref 16. Submicron particles of copper formate were prepared by ultrafine wet milling (WAB Dyno mill) of anhydrous copper formate (45 wt %; Heaven Materials, dried at 80 °C for 3 h) in dipropylene glycol monomethyl ether (DPM; 47.5 wt %; purum grade, Sigma-Aldrich), with Disperbyk 180 (7.5 wt %; BYK) as a dispersing agent. The particles were milled for 30 min at 3200 rpm. After milling, most of the dispersing agent was separated from the dispersion by centrifugation of the particles and discarding the supernatant. After the first separation, DPM was added to the particles (fourfold), and the particles were mixed and redispersed with Thinky Mixer Ar-100 (Thinky, Japan), followed by a second centrifugation. This last step was performed once more, leaving less than 1 solid wt % dispersing agent in the dispersion (determined by thermogravimetric analysis; STAR system, Mettler Toledo). After the third centrifugation, the separated copper formate particles were placed in a Thinky to separate the aggregates formed. PVP 10K (1%, Alfa Aesar) was added to the ink as a rheological agent for improving screen printing quality.

4.1.2. Preparation of Hybrid Copper Formate and 0.5 wt % CNT Dispersion Ink. This ink was prepared similarly to the above ink, with the mixing of 0.5 solid wt % HANOS ASP-100F SWCNTs with the dry copper formate before milling; thus, the CNT and copper formate were milled together. After separation of the dispersing agent, 1% PVP 10K was added as a rheological agent.

The sizes of the copper formate particles formed in both inks were evaluated by SEM and were found to be very similar, with a diameter range of 50−500 nm. The diameter of the CNTs was ∼15 nm.

4.1.3. Printing and Post Printing. The samples were manually printed by screen printing the ink with a polyester

DOI: 10.1021/acsomega.6b00478
ACS Omega 2017, 2, 573−581

mesh (100 threads/cm; NBC, Ponger 2000) on a polyimide film (125 μm; Kapton, DuPont). The printed patterns were in the shape of dog bones (as can be seen in Figure 1) with lines of length 24 mm and width 1.3 mm. After printing, the samples were dried from solvent by heating for 5 min on a hot plate at 70 °C.

4.1.4. IPL. Photonic curing was performed with a PulseForge 1200 (Novacentrix) system. The energy of single pulses was determined with the built-in bolometer. It was not possible to directly measure multiple pulses with the bolometer; according to Novacentrix, multiple pulses at 1 Hz are identical. Therefore, energy for treatment with multiple pulses was calculated by multiplying the energy for a single pulse by the number of pulses. For preliminary screening experiments, each sample (with three lines) was vertically divided into eight segments, and each segment was exposed to different IPL parameters. This was done by covering all other segments with a 1 mm metal sheet during the IPL processing of a single segment. For experiments with large samples, the entire sample was exposed to the IPL at a given setting. In both cases, three samples were prepared simultaneously. Figure S1 shows a typical sample used for quick screening of the different pulse parameters, in which the sample was divided into segments (marked by a dotted line) and each segment was separately exposed to IPL with different pulse parameters.

4.1.5. Electrical Conductance Measurements. For preliminary screening experiments (performed with small segments of a sample), the resistance was measured by two probes placed at a constant distance of 2.5 mm. For large samples, the resistance was measured by two probes placed on a single line at a distance of 22 mm. The average resistance was calculated on the basis of three measurements. For practical reasons, the examples with a resistivity value outside the measurement range (i.e., no practical conductance) were attributed a resistance of 1 000 000 Ω. The reciprocal value of the average resistance was calculated to give the conductance.

4.1.6. Sample Characterization. Profile measurements were performed with Veeco's Dektak 150. SEM and EDX imaging and measurements were performed with a MagellanT XHR SEM equipped with an EDX probe (Oxford X-Max; Oxford Instruments, U.K.). FIB was performed with Helios 600i Nanolab Dualbeam, FEI. Emission spectra of a single light pulse were obtained from Novacentrix. XRD measurements were performed using X-ray diffractometer D8 Advance of Bruker AXS.

4.1.7. Absorptance. The reflectance spectrum was measured by a CARY 5000 UV−vis−NIR spectrophotometer equipped with an integrating sphere (Varian). Samples were bar-coated on a Kapton film with a #6 bar (K-bar, England) and were measured with an aluminum sheet background to simulate the same conditions as those in the PulseForge 1200 system. Absorptance was calculated[23,28] using the $A + R + T = 1$ equation, where A is the absorptance, R is the reflectance, and T is the transmittance. R in the desired spectrum was calculated by dividing the integral of the % reflectance curve by the total area of the graph. The samples were measured with an aluminum background, so the transmittance is equal to zero and the equation is reduced to $A + R = 1$.

■ ASSOCIATED CONTENT

Supporting Information

The Supporting Information is available free of charge on the ACS Publications website at DOI: 10.1021/acsomega.6b00478.

Sample used for the screening experiment; 3D graphs; electrical conductance; SEM images (Figures S1−S4) (PDF)

■ AUTHOR INFORMATION

Corresponding Authors

*E-mail: a.yakushenko@fz-juelich.de.
*E-mail: magdassi@mail.huji.ac.il.

ORCID

Yitzchak S. Rosen: 0000-0002-6103-4410
Andreas Offenhäusser: 0000-0001-6143-2702
Shlomo Magdassi: 0000-0002-6794-0553

Author Contributions

The manuscript was written through contributions of all authors. All authors have given approval to the final version of the manuscript.

Notes

The authors declare no competing financial interest.

■ ACKNOWLEDGMENTS

This research was supported by the Ministry of Science, Technology & Space, Israel, and by the National Research Foundation, Prime Minister's Office, Singapore, under its Campus for Research Excellence and Technological Enterprise (CREATE) program. Additionally, part of the work was supported by the Helmholtz Validation Fund within the project HVF-0034 "LiveCheck". We would like to thank Elka Brauweiler-Reuters from FZJ for FIB, Dr. Vladimir Uvarov for the XRD measurements, and Asad Awadallah from the Hebrew University for his assistance with preparing the inks and the ICP samples. Finally, we would like to thank NovaCentrix, and Vahid Akhavan, for helping with the PulseForge system and for the pulse emission data.

■ REFERENCES

(1) Kwon, J.; Cho, H.; Eom, H.; Lee, H.; Suh, Y. D.; Moon, H.; Shin, J.; Hong, S.; Ko, S. H. Low-Temperature Oxidation-Free Selective Laser Sintering of Cu Nanoparticle Paste on a Polymer Substrate for the Flexible Touch Panel Applications. *ACS Appl. Mater. Interfaces* **2016**, *8*, 11575−11582.

(2) Kang, B.; Han, S.; Kim, J.; Ko, S.; Yang, M. One-step fabrication of copper electrode by laser-induced direct local reduction and agglomeration of copper oxide nanoparticle. *J. Phys. Chem. C* **2011**, *115*, 23664−23670.

(3) Joo, S. J.; Park, S. H.; Moon, C. J.; Kim, H. S. A highly reliable copper nanowire/nanoparticle ink pattern with high conductivity on flexible substrate prepared via a flash light-sintering technique. *ACS Appl. Mater. Interfaces* **2015**, *7*, 5674−5684.

(4) Han, S.; Hong, S.; Ham, J.; Yeo, J.; Lee, J.; Kang, B.; Lee, P.; Kwon, J.; Lee, S. S.; Yang, M. Y.; et al. Fast Plasmonic Laser Nanowelding for a Cu-Nanowire Percolation Network for Flexible Transparent Conductors and Stretchable Electronics. *Adv. Mater.* **2014**, *26*, 5808−5814.

(5) Suh, Y. D.; Kwon, J.; Lee, J.; Lee, H.; Jeong, S.; Kim, D.; Cho, H.; Yeo, J.; Ko, S. H. Maskless Fabrication of Highly Robust, Flexible Transparent Cu Conductor by Random Crack Network Assisted Cu Nanoparticle Patterning and Laser Sintering. *Adv. Electron. Mater.* **2016**, *2*, No. 1600277.

(6) Schroder, K. A. Mechanisms of Photonic Curing: Processing High Temperature Films on Low Temperature Substrates. In *Nanotechnology*; NSTI, 2011; Vol. 2.

(7) Niittynen, J.; Sowade, E.; Kang, H.; Baumann, R. R.; Mäntysalo, M. Comparison of laser and intense pulsed light sintering (IPL) for inkjet-printed copper nanoparticle layers. *Sci. Rep.* **2015**, *5*, No. 8832.

DOI: 10.1021/acsomega.6b00478
ACS Omega 2017, 2, 573−581

(8) Perelaer, J.; Abbel, R.; Wünscher, S.; Jani, R.; van Lammeren, T.; Schubert, U. S. Roll-to-Roll Compatible Sintering of Inkjet Printed Features by Photonic and Microwave Exposure: From Non-Conductive Ink to 40% Bulk Silver Conductivity in Less Than 15 Seconds. *Adv. Mater.* **2012**, *24*, 2620−2625.
(9) Chung, W. H.; Hwang, H. J.; Kim, H. S. Flash light sintered copper precursor/nanoparticle pattern with high electrical conductivity and low porosity for printed electronics. *Thin Solid Films* **2015**, *580*, 61−70.
(10) Park, S. H.; Kim, H. S. Flash light sintering of nickel nanoparticles for printed electronics. *Thin Solid Films* **2014**, *550*, 575−581.
(11) Paglia, F.; Vak, D.; van Embden, J.; Chesman, A. S.; Martucci, A.; Jasieniak, J. J.; Della Gaspera, E. Photonic Sintering of Copper through the Controlled Reduction of Printed CuO Nanocrystals. *ACS Appl. Mater. Interfaces* **2015**, *7*, 25473−25478.
(12) Paquet, C.; James, R.; Kell, A. J.; Mozenson, O.; Ferrigno, J.; Lafrenière, S.; Malenfant, P. R. Photosintering and electrical performance of CuO nanoparticle inks. *Org. Electron.* **2014**, *15*, 1836−1842.
(13) Draper, G. L.; Dharmadasa, R.; Staats, M. E.; Lavery, B. W.; Druffel, T. Fabrication of Elemental Copper by Intense Pulsed Light Processing of a Copper Nitrate Hydroxide Ink. *ACS Appl. Mater. Interfaces* **2015**, *7*, 16478−16485.
(14) Wang, B. Y.; Yoo, T. H.; Song, Y. W.; Lim, D. S.; Oh, Y. J. Cu ion ink for a flexible substrate and highly conductive patterning by intensive pulsed light sintering. *ACS Appl. Mater. Interfaces* **2013**, *5*, 4113−4119.
(15) Araki, T.; Sugahara, T.; Jiu, J.; Nagao, S.; Nogi, M.; Koga, H.; Uchida, H.; Shinozaki, K.; Suganuma, K. Cu salt ink formulation for printed electronics using photonic sintering. *Langmuir* **2013**, *29*, 11192−11197.
(16) Rosen, Y.; Grouchko, M.; Magdassi, S. Printing a Self-Reducing Copper Precursor on 2D and 3D Objects to Yield Copper Patterns with 50% Copper's Bulk Conductivity. *Adv. Mater. Interfaces* **2015**, *2*, No. 1400448.
(17) Galwey, A. K.; Jamieson, D.; Brown, M. E. Thermal decomposition of three crystalline modifications of anhydrous copper (II) formate. *J. Phys. Chem.* **1974**, *78*, 2664−2670.
(18) Farraj, Y.; Grouchko, M.; Magdassi, S. Self-reduction of a copper complex MOD ink for inkjet printing conductive patterns on plastics. *Chem. Commun.* **2015**, *51*, 1587−1590.
(19) Theocharous, E.; Chunnilall, C. J.; Mole, R.; Gibbs, D.; Fox, N.; Shang, N.; Howlett, G.; Jensen, B.; Taylor, R.; Reveles, J. R.; et al. The partial space qualification of a vertically aligned carbon nanotube coating on aluminium substrates for EO applications. *Opt. Express* **2014**, *22*, 7290−7307.
(20) Azoubel, S.; Cohen, R.; Magdassi, S. Wet deposition of carbon nanotube black coatings for stray light reduction in optical systems. *Surf. Coat. Technol.* **2015**, *262*, 21−25.
(21) Xia, D.; Liu, C.; Fan, S. A Solar Thermoelectric Conversion Material Based on Bi2Te3 and Carbon Nanotube Composites. *J. Phys. Chem. C* **2014**, *118*, 20826−20831.
(22) Bera, R. K.; Mhaisalkar, S. G.; Mandler, D.; Magdassi, S. Formation and performance of highly absorbing solar thermal coating based on carbon nanotubes and boehmite. *Energy Convers. Manage.* **2016**, *120*, 287−293.
(23) Bera, R. K.; Azoubel, S.; Mhaisalkar, S. G.; Magdassi, S.; Mandler, D. Fabrication of Carbon Nanotube/Indium Tin Oxide "Inverse Tandem" Absorbing Coatings with Tunable Spectral Selectivity for Solar−Thermal Applications. *Energy Technol.* **2015**, *3*, 1045−1050.
(24) Wang, Y.; Zhang, L.; Wang, P. Self-floating carbon nanotube membrane on macroporous silica substrate for highly efficient solar-driven interfacial water evaporation. *ACS Sustainable Chem. Eng.* **2016**, *4*, 1223−1230.
(25) Creighton, J. A.; Eadon, D. G. Ultraviolet−visible absorption spectra of the colloidal metallic elements. *J. Chem. Soc., Faraday Trans.* **1991**, *87*, 3881−3891.
(26) Hwang, H. J.; Chung, W. H.; Kim, H. S. In situ monitoring of flash-light sintering of copper nanoparticle ink for printed electronics. *Nanotechnology* **2012**, *23*, No. 485205.
(27) Hwang, H. J.; Joo, S.-J.; Kim, H. S. Copper Nanoparticle/Multiwalled Carbon Nanotube Composite Films with High Electrical Conductivity and Fatigue Resistance Fabricated via Flash Light Sintering. *ACS Appl. Mater. Interfaces* **2015**, *7*, 25413−25423.
(28) Selvakumar, N.; Krupanidhi, S.; Barshilia, H. C. Carbon Nanotube-Based Tandem Absorber with Tunable Spectral Selectivity: Transition from Near-Perfect Blackbody Absorber to Solar Selective Absorber. *Adv. Mater.* **2014**, *26*, 2552−2557.

DOI: 10.1021/acsomega.6b00478
ACS Omega 2017, 2, 573−581